

# Buckling Analysis of Rectangular Laminated Composite Plates With An Edge Delamination Under Compressive Load

M. A. Kouchakzadeh<sup>1</sup>

*A buckling analysis of rectangular laminated composite plates with an edge delamination under in-plane compressive loading is performed using the finite element method. Such plates may be considered as simplified models of stiffener plates of a stiffened panel. The buckling load and buckling mode are obtained by solving an eigenproblem. In an unconstrained analysis, physically inadmissible modes may appear because of the overlap between separated sublaminates in the delaminated region. To eliminate overlap, constraints are added iteratively on the entire overlapped area using penalty function method. The validity and superiority of the analysis method in predicting buckling load and buckling mode are shown in comparison with the experimental and analytical results available in the literature. Numerical results show the effect of delamination width and depth and boundary conditions on the buckling load.*

## INTRODUCTION

Delamination is one of the most serious failure modes of laminated composite plates and can severely reduce their compressive strength. It may arise because of imperfections in the production process. A common cause is the air bubble trapped between the plies of laminated plate at the time of production resulting in a circular or elliptical embedded delamination.

Delamination can be the consequence of the low velocity impact of foreign objects, which usually appear as multiple embedded delaminations through out the thickness of the laminate. In addition, delamination may arise because of interlaminar stress at the interfaces of the plies. This is particularly important when the laminated composite plate is subjected to periodic load (fatigue). It is known that complex interlaminar stress distributions arise at the interface of the plies of laminated plates, especially near the free edges. The stress components change rapidly near the edge and can induce 'edge delamination'.

Considerable research has been conducted to know more about delaminations and their effects on the structure. A single one-dimensional through-the-width delamination is the simplest model, which was

investigated by Chai *et.al.* [1]. They were perhaps the pioneers to characterize delamination buckling models by delamination thickness and the number of delaminations through the thickness. Other researchers [2-5] investigated similar through-the-width delamination models. Embedded delaminations with various shapes were investigated as more practical models [6-12]. Another delamination model with practical interest is the edge delamination, which is investigated by Suemasu *et.al.* [13,14]. They have conducted an experimental and analytical investigation on the compressive buckling behavior of orthotropic plates with an edge delamination.

To investigate the response of the delaminated composite plate under in-plane compressive loading, a buckling analysis is required. This analysis may be carried out in two ways, one is to follow the history of load-displacement variations in a non-linear analysis, the other is to solve an eigenproblem. The former method provides us with buckling load along with displacement information; however, the later one results in just buckling load and mode. Usually the chief concern of designers is the buckling load. In this case, the eigenproblem method is the proper selection because of its relative simplicity and speed.

Unconstrained buckling analysis of delaminated composite plates leads to physically inadmissible re-

---

1. Assistant Professor, Dept. of Aerospace Eng., Sharif Univ. of Tech., Tehran, Iran, Email: mak@sharif.edu.

sults in some cases due to overlap. Searching for physically admissible result requires constraints to be added in a contact analysis. There are two basic and well-known methods for insertion of such constraints, ‘‘Lagrange multiplier method’’ and ‘‘penalty function method’’. The penalty function method is commonly used for contact problems. As compared to the Lagrange multiplier method, the penalty function method can give only an approximate solution, however, in the case of penalty function method no zero is encountered on the diagonal components of the stiffness matrix, and the number of unknowns does not increase.

Although delamination buckling problem has been already investigated extensively for different models, the contact problem seems to need further considerations. As an example, the specific model of edge delamination is considered by Suemasu *et.al.* [13]; however, they report a problem in matching the results obtained by experiment and analysis (after inclusion of constraint) for buckling mode in one case. They consider just one constrained point and add imaginary springs at that point to prevent overlap.

This study examines the effect of edge delamination on the compressive buckling of rectangular laminated composite plates. Buckling load and mode are obtained by solving an eigenproblem using finite element method. Constraints preventing overlap in the form of imaginary springs with suitable stiffness are added for all points in the overlapped area by penalty function method through iterations. This is in contrast to the method used in reference [13], where a single constrained point is used at the center of the overlapped area. In addition, here we choose the stiffness of the imaginary springs by considering the overlap depth and elastic properties of the structure at each point. The effect of delamination width and depth and boundary conditions on the buckling load and buckling mode of delaminated plate is investigated and the results are compared to those in [13]. Predicted results coincide with the experimental results of the mentioned reference for the case that an inconsistency between analytical and experimental result is reported.

## ANALYTICAL MODEL

A rectangular laminated composite plate under in-plane compressive loading with an edge delamination as shown in Figure 1 is considered. Each ply of the plate can have unidirectional material properties. The delaminated side is free and other three sides of the plate are considered simply supported or clamped in different cases. A practical problem may involve multiple edge delaminations with different widths. However, we consider a single edge delamination with constant width at the free edge of the plate to simplify the model. This enables us to investigate the effect of

parameters such as delamination width and depth, and boundary conditions on the buckling load and mode of the plate.

The delamination divides the base plate in the delaminated area into two regions, which are called upper and lower sublaminates with respect to the direction of the  $z$ -axis. In lamination sequence notation, the zero degree refers to a ply with fibers aligned in the load direction. Nondimensional delamination width and depth are defined as  $\alpha = c/a$  and  $\gamma = h/H$ , respectively.

## BUCKLING ANALYSIS AND CONTACT ANALYSIS

### Buckling analysis

The Mindlin plate theory is used to obtain fundamental equations of the rectangular laminated composite plate with an edge delamination shown in Figure 1. Finite element method is employed for the buckling analysis of this plate. Basic equation for the plate buckling analysis is:

$$[K]\{\phi\} = \lambda[K_G]\{\phi\}, \quad (1)$$

where  $[K]$  and  $[K_G]$  are elastic and geometric stiffness matrices of structure, and  $\{\phi\}$  is the generalized global displacement vector. Bending-stretching coupling is considered in calculation of stiffness matrices. This eigenproblem is solved by a simultaneous iteration method [15]. The smallest eigenvalue  $\lambda_1$  is the buckling load  $N_{cr}$  and its corresponding eigenvector  $\{\phi_1\}$  represents the buckling mode.

Generally, a laminated composite plate may be unsymmetric about the mid-plane. Even when we use a symmetric laminate as the base plate, the upper and lower sublaminates may become unsymmetric due to delamination. In these cases, we should pay careful attention to the position of in-plane load applied at the edges. If we apply the load as usual at the mid-plane, because of the bending-stretching coupling, displacement in the lateral direction appears from the beginning of the load application and we will not have a bifurcation buckling. However, by applying sufficient moments at the loading edges and/or considering proper boundary conditions we can make a model closer to the real problem and obtain the buckling load.

Consider the case of applying in-plane compressive load on the edge of a plate such that the displace-

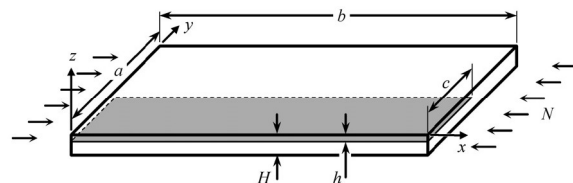


**Figure 1.** Rectangular laminated composite plate with an edge delamination.

ment of the points on the edge in the load direction is uniform (the plate does not bend). The resultant of such a load will be on the neutral axis, which is not coincident with the mid-plane for unsymmetric laminates. In our model, we should find this lateral position and apply the in-plane load there. This position for unsymmetric laminates may be obtained easily by using the parallel axis theorem explained by Tsai and Hahn [16]. Using this theorem, we can obtain the stiffness terms of the laminate when our reference line is transferred by a distance  $d$  along the  $z$ -axis from the mid-plane.

$$\begin{aligned} A'_{ij} &= A_{ij} \\ B'_{ij} &= B_{ij} + dA_{ij} \\ D'_{ij} &= D_{ij} + 2dB_{ij} + d^2A_{ij}. \end{aligned} \quad (2)$$

Here  $A'_{ij}$ ,  $B'_{ij}$  and  $D'_{ij}$  are the extensional, coupling and bending stiffness terms with view of the transformed axis, and  $A_{ij}$ ,  $B_{ij}$  and  $D_{ij}$  are similar terms with view of the mid-plane. For example, if we have an unsymmetric cross-ply sublaminate under in-plane compressive loading in the  $x$  direction, the proper lateral position for the application of the load can be obtained by setting  $B'_{11} = 0$ , resulting

$$d = -\frac{B_{11}}{A_{11}}. \quad (3)$$

Applying the load at this lateral position, or equivalently applying the usual load at the mid-plane plus equivalent moment, can prevent bending in the  $x$  direction. However, because of the Poisson effect there will be a bending in the  $y$  direction too, changing the shape of the plate to a curved panel. Our investigation on approximate deflection near the buckling load using a linear static analysis indicates that this bending is very small and is ignored in this analysis.

#### Displacement conditions at intersection of sublaminates and base plate

Each sublaminate in the delaminated region is considered as a separate Mindlin plate. In the finite element mesh as shown in Figure 2, we consider separate meshes for the upper and lower sublaminates and connect them at the intersection of sublaminates and base plate ( $y = c$ ) by using displacement conditions similar to the Mindlin plate displacements. For example the displacements of point  $j$  on the upper sublaminate is related to the displacements of point  $i$  on the base plate as

$$\begin{aligned} u_j &= u_i - z_j\theta_{xi}, & v_j &= v_i - z_j\theta_{yi} \\ w_j &= w_i, & \theta_{xj} &= \theta_{xi}, & \theta_{yj} &= \theta_{yi}, \end{aligned} \quad (4)$$

where  $u$ ,  $v$ ,  $w$  are translations in the  $x$ ,  $y$ ,  $z$  directions and  $\theta_x$ ,  $\theta_y$  are rotations in the  $xz$  and  $yz$

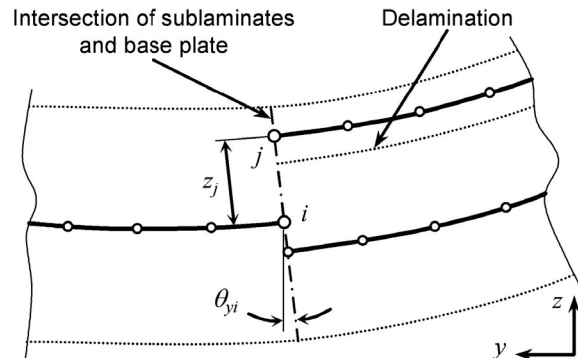


**Figure 2.** Displacement conditions at intersection of sublaminates and base plate.

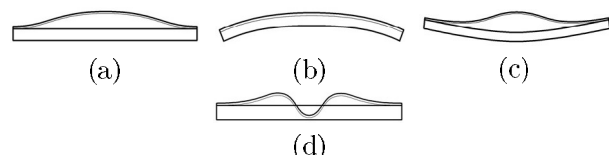


**Figure 3.** Admissible and inadmissible buckling modes of a delaminated plate.

planes. Relations similar to Eq. (4) are considered as constraints on all points on the upper and lower sublaminates at  $y = c$ , and are included in the analysis by using the penalty function method.

#### Contact analysis

A delaminated plate buckles in local, global or mixed buckling modes under in-plane compressive loading as shown in Figures 3(a), 3(b) and 3(c), respectively. An unconstrained analysis of delaminated plates leads to physically inadmissible results in some cases due to overlap as shown in Figure 3(d). Searching for physically admissible results requires constraints to be included in the analysis, thereby preventing interpenetration. In this study we use the penalty function method for this purpose.

The overlap spreads over an area, which may not be small in all cases. Adding a single constraint at the center of overlapped area is not sufficient since the deformation around the point changes after including constraint and we may have overlaps at nearby points again. To prevent this, we should add constraints on all overlapped areas rather than a single point at its center. In this study, we use the finite element method and consider the plate as discrete points. Therefore, we add constraints for all discrete points in the overlapped area. The constraint value for each point is calculated by considering the elastic properties and overlap depth at that point.

#### Penalty function method and fictitious springs

The penalty function method is a common method to include constraints in the analysis. The problem is to

find the solution by minimizing the potential energy of the structure  $U(\phi)$ , subjected to some constraints. In the penalty function method, we make a pseudo-objective function  $U$ , by adding a penalty function to the original objective function in the form

$$U(\phi, r_p) = U(\phi) + r_p P(\phi). \quad (5)$$

Here,  $P(\phi)$  is the penalty function, and  $r_p$  is a multiplier determining the magnitude of penalty. There are different variations of the penalty function method which determine the shape of the penalty function  $P(\phi)$ . In ‘‘exterior penalty function method’’ we consider the square of the active constraints as the penalty function.

In overlap problems, the constraint is:

$${}^{ij}\delta \geq 0, \quad (6)$$

where  ${}^{ij}\delta$  is the gap between any pair of points  $i$  and  $j$  on the upper and lower sublaminates in the overlapped area as shown in Figure 4. Considering this constraint and representing  $r_p$  with  $k^*/2$ , the pseudo-objective function is given as:

$$U(\phi, k^*) = U(\phi) + \frac{1}{2} {}^{ij}k^* {}^{ij}\delta^2. \quad (7)$$

Representing the pseudo-objective function in this form gives a physical meaning to the constraint. The constraint works as a fictitious spring with a stiffness of  ${}^{ij}k^*$  inserted between points  $i$  and  $j$  on the upper and lower sublaminates in the overlapped area to restrict their relative displacements and hence eliminate the overlap. It should be mentioned again that the second term in the right hand side of Eq. (7) should be added for each pair of discrete points in the overlapped area. In practice, we add constraints by adding the effect of these fictitious springs to the stiffness matrix. We should find suitable values for the stiffness of fictitious springs. It is necessary to eliminate the overlap in an iterative process by reducing the allowable overlap through iterations.

#### Calculation of $k^*$

An efficient method for the calculation of  $k^*$ , which considers the elastic properties of the structure and overlap depth at each position, is introduced by Sekine *et.al.* [12]. The final results of that study are reproduced here. As an example, consider the fictitious

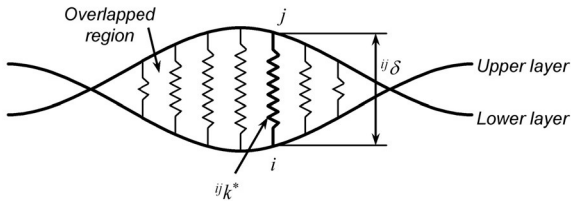


**Figure 4.** Insertion of fictitious spring to eliminate overlap.

spring  ${}^{ij}k^*$  between points  $i$  and  $j$  on the upper and lower sublaminates as shown in Figure 4. To obtain the suitable value of  ${}^{ij}k^*$  we extract two equations related to the lateral displacement of points  $i$  and  $j$  from Eq. (1), and include the effect of the unknown fictitious spring, which restricts the overlap at points  $i$  and  $j$ . After some manipulations we can find the stiffness of the fictitious spring to be inserted between these points as:

$${}^{ij}k^* = \frac{(k_{mm} + k_{nn})P_n - (k_{mn} + k_{nn})P_m}{\frac{{}^{ij}\delta}{1+r}(k_{mm} + 2k_{mn} + k_{nn})} + \frac{\frac{{}^{ij}\delta}{1+r}(k_{mn}^2 - k_{mm}k_{nn})}{{}^{ij}\delta(k_{mm} + 2k_{mn} + k_{nn})}, \quad (8)$$

where

$$P_m = \lambda \sum_{l=1}^N k_{Gml} w_l - \sum_{\substack{l=1 \\ (l \neq m, l \neq n)}}^N k_{ml} w_l, \quad (9)$$

$$P_n = \lambda \sum_{l=1}^N k_{Gnl} w_l - \sum_{\substack{l=1 \\ (l \neq m, l \neq n)}}^N k_{nl} w_l \quad (10)$$

Here, lateral displacements of points  $i$  and  $j$  are the  $m$ -th and  $n$ -th elements of the global displacement vector,  $k$  and  $k_G$  are the elements of elastic and geometric stiffness matrices,  $N$  is the total degrees of freedom in the structure,  ${}^{ij}\delta = w_n - w_m$  is the overlap depth between points  $i$  and  $j$ , and  $r$  is an initially small value which is increased in each iteration. To eliminate overlap, we should find the stiffness of fictitious springs for all points in the overlapped area using Eq. (8) and add their effects in the stiffness matrix. The overlap can be reduced as much as required by increasing the value of  $r$  through iterations. The initial value for  $r$  and its increasing pace control the convergence rate. Choosing an initial value of 0.00001 for  $r$  and multiplying it by 3 may form a good convergence pattern. The maximum overlap is the convergence criterion, where iteration will be terminated if the maximum overlap is smaller than a preset small value.

One point should be considered when we use this method, and that is multiplying  $\phi_1$ , the eigenvector corresponding to the smallest eigenvalue of the eigenproblem in Eq. (1), by a minus value changes the overlapped area, although both of them are valid eigenvectors. To determine the overlap region we use Rayleigh quotient to guess the buckling load of the next iteration and follow the mode corresponding to the lower buckling load.

$$\lambda + \Delta\lambda = \frac{\phi_1^T (K + K^*) \phi_1}{\phi_1^T K_G \phi_1}, \quad (11)$$

$$\Delta\lambda = \frac{\phi_1^T K^* \phi_1}{\phi_1^T K_G \phi_1}. \quad (12)$$

Here,  $\Delta\lambda$  is the buckling load increment due to introduction of fictitious springs and  $K^*$  is a matrix containing all fictitious springs in proper positions. We will have two different  $K^*$  s for  $\phi_1$  and  $-\phi_1$ . Therefore, we obtain two different  $\Delta\lambda$  values. The mode corresponding to the smaller  $\Delta\lambda$  is considered as the buckling mode.

## RESULTS AND DISCUSSION

The numerical results are obtained by using the finite element method. In this study, we use a regular mesh of eight-noded isoparametric Mindlin plate elements with five degrees of freedom per node. In the delaminated region, two series of elements on top of each other are considered. Displacements of the points at the intersection of sublaminates and base plate are constrained as explained earlier. To be sure about the reliability of the results, a convergence check is performed and it is concluded that a mesh made of 192 elements, 683 points, with 2953 degrees of freedom gives acceptable results.

### Comparison with available results

To show the validity of the present results, a comparison is made with the experimental and analytical results presented by Suemasu *et.al.* [13]. As the first step, to be sure about the buckling analysis, the buckling load of the intact plate is compared to the experimental results. The material used in the experiment is plain woven carbon fiber-reinforced composite (Toray T300/epoxy, Vf  $\approx$ 50%) with properties of material A in Table 1. The plate has sixteen plies,  $H=3.49$  mm,  $a=65$  mm, and  $b=240$  mm. Three sides of the plate are simply supported and other side which is along the length of the plate is free. The simply support line along the length of the plate is placed 5 mm inside the plate. The experimental buckling load for the intact plate has been 680 kgf (6664 N). The present method results in 6570 N, which is about 1.4 percent lower than the previous results.

In the next step, the results for the case of  $\alpha=1/2$ ,  $\gamma=2/16$  are investigated. Here, plate dimensions are  $H=3.49$  mm,  $a=60$  mm, and  $b=240$  mm and the simply supported line along the length of the plate is placed exactly on the edge. The analytical results for the buckling mode of this case are shown in reference [13] and it is said that this buckling mode does not coincide with the experimental one, which closes at

**Table 1.** Material properties.

| Material | $E_{11}$ (GPa) | $E_{22}$ (GPa) | $G_{12}$ (GPa) | $\nu_{12}$ |
|----------|----------------|----------------|----------------|------------|
| A        | 61.7           | 61.7           | 5.17           | 0.046      |
| B        | 181            | 10.3           | 7.17           | 0.28       |

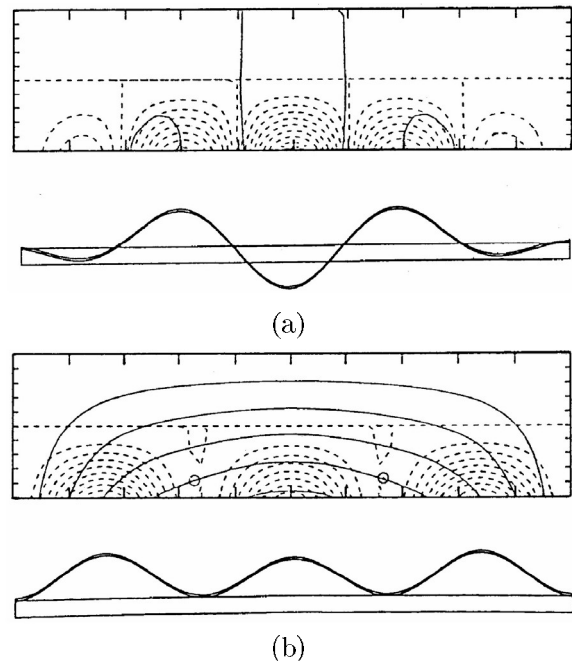


**Figure 5.** Buckling modes for  $\alpha=1/2$ ,  $\gamma=2/16$  by Suemasu *et.al.* [13] (a) Inadmissible solution, (b) Admissible solution.

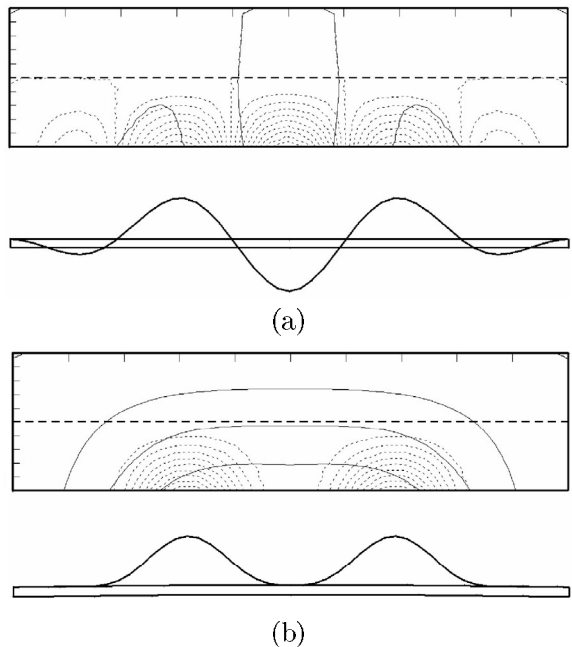


**Figure 6.** Buckling modes for  $\alpha=1/2$ ,  $\gamma=2/16$  Present analysis (a) Inadmissible solution, (b) Admissible solution.

its center. The inadmissible and admissible buckling modes obtained there are shown in Figures 5a and 5b. Dashed and solid lines show the contour lines of deflection of the upper and lower sublaminates in different scales, respectively. In [13] to eliminate overlap, only one constrained point is introduced at the center of the overlapped area.

In the present study, I add constraints on entire overlapped area and increase the penalty value through

iterations, as described earlier. The buckling modes of the same case when analyzed with the present method, are shown in Figures 6a and 6b. As it is expected from the experimental results, the gap between the sublaminates closes at the center.

Figure 7 shows buckling loads obtained by the present study and those of Suemasu *et.al.* [13]. The normalizing factor for buckling load in Figure 7 is  $N_1=5.83 \times 10^3$  N, which is the buckling load of an intact plate. This figure shows that buckling load decreases by increasing the delamination width  $\alpha$ . For small delamination width, buckling load is high, as global buckling mode is governing. As we increase  $\alpha$  and pass about  $\alpha=0.35$ , buckling load decreases sharply with appearance of mixed and local buckling modes. The reduction of buckling load in the global mode phase is almost linearly proportional to  $\alpha$ . The slope of this line however, is slightly different in the two studies.

Figure 7 also shows that in the case of  $\alpha=1/2$ ,  $\gamma=2/16$ , there is another local buckling mode with a buckling load very close to the first one. This buckling mode (after elimination of overlap) includes three waves and opens at the center, similar to Figure 5(b). Probably, the insertion of a single severe constraint in [13] has caused a change in the buckling mode. The second mode in the current analysis has appeared as the first mode in [13].

### Effect of different parameters

A rectangular laminated composite plate with a single edge delamination as shown in Figure 1 is used to solve some numerical examples. Material properties are B in Table 1. The plate is made of sixteen plies with  $[0/90]_{4s}$  lamination sequence, and the plate dimensions are  $H=3.40$  mm,  $a=60$  mm, and  $b=120$  mm. Various cases are analyzed to investigate the effects of delamination width and depth and boundary conditions on the buckling load.

#### Effect of delamination width and depth

A rectangular cross-ply laminated composite plate as defined above is considered. The delaminated side is free and other three sides of the plate are simply

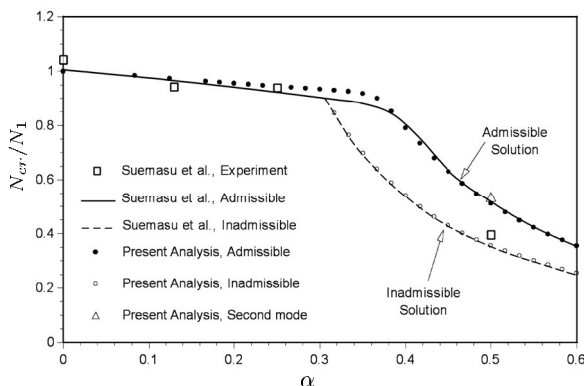


Figure 7. Buckling loads for  $\gamma=2/16$

supported. As explained earlier, presence of delamination can result in unsymmetric sublaminates. In this case we should be careful about the boundary and load conditions to have a bifurcation buckling problem. In the simply supported case, extra moments at the loading edges are needed. Here we calculate them using Eq. (3) for each sublamate.

Figure 8 shows the buckling loads for various delamination widths  $\alpha$  when delamination is placed at different depths  $\gamma$ . For example,  $\gamma=1/16$  refers to a delamination placed at the interface of the first and second plies and  $\gamma=8/16$  represents a delamination placed at the mid-plane. Solid and dashed lines show the admissible and inadmissible results respectively. The normalizing factor for the buckling load is  $N_2=1.94 \times 10^4$  N, which is the buckling load of an intact plate.

For delamination with very small width ( $\alpha < 0.06$ ), we see global buckling modes with buckling loads close to the buckling load of the intact plate. Increasing the width of the delamination results in appearance of mixed and local buckling modes with lower buckling loads. The delamination width, which provokes this mode change, depends on the delamination depth  $\gamma$ . For thin delaminations ( $\gamma \leq 2/16$ ), the mode changes sharply from global mode to the local mode and buckling load drops rapidly. However, in thicker delaminations the change of buckling mode is relatively smooth. For delaminations placed deep inside the thickness ( $\gamma \geq 5/16$ ), no local buckling occurs and we see only global and mixed buckling loads with relatively high buckling loads.

The effect of constraints on the buckling load is visible in Figure 8. The overlap occurs in local or mixed buckling modes. Therefore, there is no considerable effect of constraints for deep delaminations ( $\gamma > 4/16$ ). For thin delaminations, the effect of the constraints appear when the global mode changes to mixed mode as  $\alpha$  increases. This effect disappears in wider delaminations because the delaminated section is larger and overlap may be eliminated easily. A small cusp can be seen around  $\alpha=0.36$  in the curve for  $\gamma=3/16$ . This is because the buckling mode is changing at this point from a two-wave form to a one-wave form as  $\alpha$  increases. After change of the buckling mode to a one-wave form, the buckling load decreases more rapidly as can be seen from the graph.

#### Effect of boundary conditions

To examine the effect of boundary conditions, two cases are considered. In one case, which we call simply supported, the edge with delamination is free and other three sides are simply supported. The other case, which is called clamped, has one free edge with delamination, its opposite side is simply supported and load-bearing sides are clamped.

Figure 9 shows the buckling load of the laminate under simply-supported and clamped boundary conditions. The normalizing factor is  $N_2=1.94 \times 10^4$  N, which is the buckling load of an intact simply supported plate. For small delamination widths there is a great difference between the clamped and simply supported plates. This is because the global buckling load of clamped plate is considerably higher than the global buckling load of the simply supported plate. However, as  $\alpha$  increases the difference decreases and actually for thin delamination we can not see any difference between the buckling load of the cases. This means that the boundary condition has a very limited effect on the buckling of thin and wide delaminations where the local buckling mode is governing.

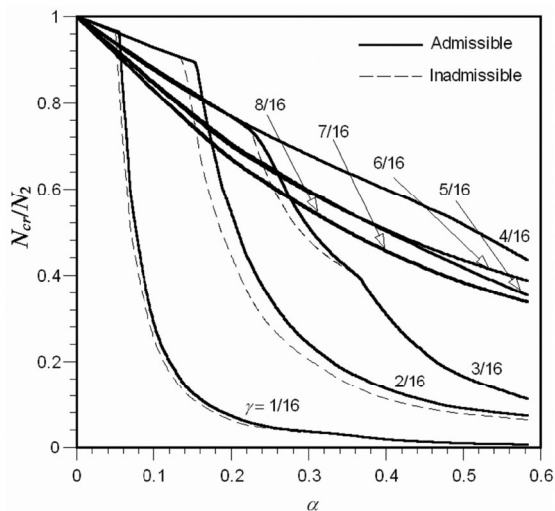


Figure 8. Effect of delamination width and depth

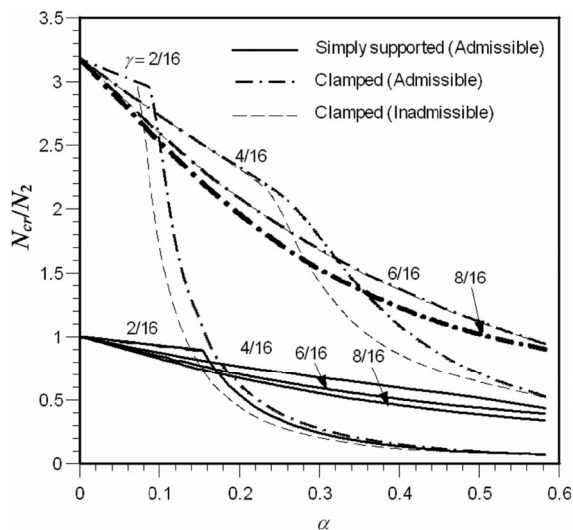


Figure 9. Effect of boundary conditions.

## CONCLUSIONS

The finite element method was used to evaluate the buckling load and mode of rectangular laminated composite plates with an edge delamination subjected to in-plane compressive loading. To eliminate possible overlap, penalty function method was employed to add constraints on the entire overlapped area. The validity of the results was proved in light of available experimental results. The effect of parameters such as delamination width and depth and boundary conditions of the plate on its response are investigated. It is found that:

- Buckling load decreases as delamination width increases. This relation is nearly linear in the global buckling mode phase. Depending on the delamination depth, mixed and local modes appear somewhere as delamination width increases.
- Appearance of mixed and local modes decreases the buckling load. The thinner the delamination, the sharper the decrease.
- Ignoring the overlap problem may result in 40% (or even more) error margin in the buckling load of the mixed and local modes. There is no considerable effect in global mode.
- The constraints used to eliminate overlap should be selected carefully, or we may find incorrect buckling modes. It is suggested to impose the constraints on all of the nodes in the overlapped area.
- The main effect of the boundary conditions is in the global and mixed modes, *i.e.* in thick and small width delaminations.

## REFERENCES

1. Chai H., Babcock C. D., Knauss W. G., "One Dimensional Modelling of Failure in Laminated Plates by Delamination Buckling", *International Journal of Solids and Structures*, **17**, PP 1069-1083(1981).
2. Simitzes G. J., Sallam S., Yin W. L., "Effect of Delamination of Axially Loaded Homogeneous Laminated Plates", *AIAA Journal*, **23**, PP 1437-1444(1985).
3. Kardomateas G. A., Schmueser D. W., "Buckling and Postbuckling of Delaminated Composites Under Compressive Loads Including Transverse Shear Effects", *AIAA Journal*, **26**, PP 337-343(1988).
4. Kapania R. K., Wolfe D. R., "Buckling of Axially Loaded Beam-Plate with Multiple Delaminations", *Transactions of ASME, Journal of Pressure Vessel Technology*, **111**, PP 151-158(1989).
5. Lee J., Gurdal Z., Griffin O. H. Jr., "Layer-Wise Approach for the Bifurcation Problem in Laminated Composites with Delaminations", *AIAA Journal*, **31**, PP 331-338(1993).
6. Chai H., Babcock C. D., "Two-Dimensional Modelling of Compressive Failure in Delaminated Laminates", *Journal of Composite Materials*, **19**, PP 67-98(1985).

7. Chai H., "Buckling and Post-Buckling Behavior of Elliptical Plates: Part 1- Analysis, Part 2- Results", *Transactions of ASME, Journal of Applied Mechanics*, **57**, PP 981-994(1990).
8. Mukherjee Y. X., Xie Z., Ingrassia A. R., "Delamination Buckling of Laminated Plates", *International Journal of Numerical Methods in Engineering*, **32**, PP 1321-1337(1991).
9. Whitcomb J. D., "Analysis of a Laminate with a Post-buckled Embedded Delamination, Including Contact Effects", *Journal of Composite Materials*, **26**, PP 1523-1535(1992).
10. Yeh M. K., Tan C. M., "Buckling of Elliptically Delaminated Composite Plates", *Journal of Composite Materials*, **28**, PP 36-52(1994).
11. Wang J. T. S., Cheng S. H., Lin C. C., "Local Buckling of Delaminated Beams and Plates Using Continuous Analysis", *Journal of Composite Materials*, **29**, PP 1374-1402(1995).
12. Sekine H., Hu N., Kouchakzadeh M. A., "Buckling Analysis of Elliptically Delaminated Composite Laminates with Consideration of Partial Closure of Delamination", *Journal of Composite Materials*, **34**, PP 551-574(2000).
13. Suemasu H., Gozu K., Hayashi K., "Compressive Buckling of Rectangular Composite Plates With a Free-Edge Delamination", *AIAA Journal*, **33**, PP 312-319(1995).
14. Suemasu H., Kawauchi M., Gozu K., Hayashi K., Ishikawa T., "Effects of a Free Edge Delamination on Buckling of Rectangular Composite Plates with Two Fixed Loading and one Simply-Supported Side Edges", *Advanced Composite Materials*, **5**, PP 185-200(1996).
15. Corr R. B., Jennings A., "A Simultaneous Iteration Algorithm for Symmetric Eigenvalue Problems", *International Journal of Numerical Methods in Engineering*, **10**, PP 647-663(1976).
16. Tsai S. W., Hahn H. T., *Introduction to Composite Materials*, Technomic Pub. Co., (1980).